ORIGINAL ARTICLE

Non-invasive Three-dimensional Bone–Vessel Image Fusion using Black Bone MRI based on FIESTA-C

Tetsuji Hayashi, RT[1]; Noriyuki Fujima, MD, PhD[2]; Akiyoshi Hamaguchi, RT[1]; Toshihide Masuzuka, RT[1]; Kazuhiro Hida, RT[1]; Shuuichi Kodera, RT[2]

[1] Department of Radiology, Sapporo Azabu Neurosurgical Hospital, Sapporo, Japan

[2] Department of Diagnostic and Interventional Radiology, Hokkaido University Hospital, Sapporo, Japan

Corresponding Author

Noriyuki Fujima

Department of Diagnostic and Interventional Radiology, Hokkaido University Hospital

N15, W7, Kita-Ku, Sapporo 060-8638, Japan

Phone: +81-11-706-5977, Fax: +81-11-706-7876

E-mail: Noriyuki.Fujima@mb9.seikyou.ne.jp

Acknowledgement

None

Competing interests;

The authors declare that they have no competing interests.

Funding;

This research received no specific grant from any funding agency in the public, commercial, or not-for-profit sectors.

ABSTRACT

Aim: To evaluate the image quality of bone–vessel fused volume-rendering (VR) images reconstructed by magnetic resonance (MR) three-dimensional “black bone” imaging based on the fast imaging employing steady-state acquisition cycled phases (FIESTA-C) sequence and time of flight MR angiography (TOF-MRA).

Materials and Methods: Seventeen patients were analyzed in this retrospective study. All patients underwent both MR scanning including FIESTA-C and TOF-MRA and computed tomography-angiography (CTA). MR- and CT-based bone–vessel VR images were respectively reconstructed. Visual depictions of frontal and parietal branches from the superficial temporal artery (STA) were independently scored by three experienced radiological technologists using a four-grade system.

Results: In the visual evaluation, the scores of the both right and left frontal branches in MR based VR image were significantly larger those in CT ($p<0.01$, respectively). The scores of both the right and left parietal branches tended to be larger in in MR-based than that in CT-based VR imaging, but weren’t significantly so ($p=0.06$, 0.13 respectively). In the inter-observer agreement analysis, κ values were all good (range: 0.6–0.76) for STA branch evaluation in MR-based VR images.

Conclusion: MR bone–vessel fused VR imaging can non-invasively depict STA frontal

branches with better visibility compared to the CT-based VR imaging. This technique may be useful for the preoperative evaluation of donor branches for STA-MCA bypass surgery.

Non-invasive Three-dimensional Bone–Vessel Image Fusion using Black Bone MRI based on FIESTA-C

Abbreviations

3D: Three-dimensional

b-SSFP : balanced steady-state free procession

CT: computed tomography

CTA: computed tomography-angiography

EC-IC: External carotid artery-internal carotid artery

ECA: external carotid artery

FA: flip angle

FIESTA-C: Fast Imaging Employing Steady-state Acquisition Cycled Phases

MCA: middle cerebral artery

MRA: magnetic resonance angiography

MRI: magnetic resonance imaging

SNR: signal-to-noise ratio

STA: superficial temporal artery

TOF: time of flight

VR: volume-rendering

Introduction

External carotid artery-internal carotid artery (EC-IC) bypass is an important treatment method in cases of intracranial vascular occlusion or stenosis such as Moyamoya disease [1-3]. Particularly, superficial temporal artery (STA)-middle cerebral artery (MCA) bypass surgery is frequently performed. Three-dimensional (3D) computed tomography-angiography (CTA) is usually used to evaluate potential donor branches of the external carotid artery for EC-IC bypass using reconstruction of the volume-rendering (VR) image of arteries running along the surface of the skull. However, poor depiction of external carotid artery (ECA) branches in CTA is sometimes experienced, probably because of the mismatch between image acquisitions and transit delay in contrast agent and the beam hardening effect due to the high computed tomography (CT) value of the skull. ECA branches are particularly sensitive to these effects because these arteries are usually running along the surface of the skull, resulting in their poor depiction on imaging. Furthermore, there are several risks related to the invasiveness of CTA: allergies to iodine contrast agent, extravascular leak due to too-rapid injection and radiation exposure [4].

In contrast, time of flight (TOF) magnetic resonance angiography (MRA) does well at visualizing intra- and extracranial arteries non-invasively. In recent decades, the

image quality and arterial depiction of TOF-MRA has been developing [5], with the broad spread of 3-Tesla magnetic resonance imaging (MRI) units worldwide. Using arteries that are well depicted by TOF-MRA, the preoperative evaluation of intra- and extra-cranial arteries for EC-IC bypass surgery can be non-invasively performed. However, there remains one problem: the reconstruction of VR images with both vessel and bone depiction is difficult using MRI only, because MRI is not suitable for composing 3D skull images. To solve this problem, we focused on previous studies that have performed 3D image reconstruction of the skull utilizing the low signal intensity of the bone acquired by gradient echo sequence, also known as the “black bone” MRI [6-11].

The aim of this study was to evaluate the clinical utility of bone–vessel VR images reconstructed by MR 3D skull imaging and TOF-MRA.

Materials and Methods

Subjects

The protocol of this retrospective study was approved by our institutional review board, and written informed consent was waived. We evaluated all 17 patients

who were surgically treated with EC-IC bypass at our hospital from November 2015 to May 2016. Patient characteristics were as follows: 7 males and 10 females, average age 51.14 (range, 25–67) years. In the pre-operative evaluation, all patients received a magnetic resonance imaging (MRI) examination including 3D Fast Imaging Employing Steady-state Acquisition Cycled Phases (FIESTA-C) and TOF-MRA. All patients also received CTA before the pre-operative MRI evaluation mentioned above.

Imaging protocol

All MR scanning was performed using a 3.0-Tesla magnet (Discovery MR 750, GE Healthcare, Milwaukee, MI, USA) with a 12-inch head neck and spine coil. Post processing of VR reconstruction was performed by ZIO Workstation (ZIOSOFT Inc., Tokyo, Japan). In previous reports, so-called “black-bone” MRI was developed using the 3D volume of proton-weighted image contrast for good depiction of bone tissue with low signal intensity [6-9]. In the current study, we selected black-bone MRI using the FIESTA-C sequence in the acquisition of raw images for both the short scanning time and high signal-to-noise ratio (SNR). In the image acquisition, because the bone marrow tissue presenting in the “black bone” with high signal intensity weakens its emphasis, the marrow fat signal, especially in skull bone with thin cortex, such as the

77 temporal bone, may result in poor depiction of black bone after VR processing, given
78 the high signal intensity of marrow fat. Therefore, it was necessary to suppress the high
79 signal of marrow fat as possible. In addition, we focused on preventing the banding
80 artifacts which are specific to the balanced steady-state free procession (b-SSFP)
81 sequence (12, 13). In the current study, we used the imaging parameters of shortest TR
82 and TE; additionally, an intermediate-value flip angle (FA) of 17° was selected to obtain
83 images with only intermediate marrow fat signal and to reduce the degree of the
84 banding artifacts (12, 13). Details of the imaging parameters of black-bone MRI used in
85 the current study are summarized in Table. 1. TOF-MRA was also obtained with the
86 same scanning with following parameters: TR 23 ms, TE 3.4 ms, flip angle 18°, field of
87 view 20 cm, matrix 448 × 224, slice thickness 1.0 mm, number of slices 168. In
88 addition, CTA was performed in all patients using a 64-slice multi-detector-row CT
89 scanner (Light Speed VCT Vision, GE Healthcare, Milwaukee, MI, USA). The settings
90 used for CT scanning were as follows: 120 kVp, 800 mA, 0.4 s/rot, and helical pitch =
91 0.53. Before the scanning, 350 mg iodine contrast agent (Iopamidol, 370 mg I/ml,
92 Bayer, Osaka) was venously injected by power injector with the flow rate of 29.2
93 mgI/kg/sec (12-sec injection). Arterial arrival of contrast agent for the determination of
94 acquisition timing was adjusted for the depiction of intracranial arteries using a bolus

tracking technique with target point of distal internal carotid artery. All scanning was performed to include the whole brain in its scan range.

Post processing

We performed post processing to create 3D bone–vessel fusion images from TOF-MRA and black-bone images obtained by 3D FIESTA-C sequence in all patients by the VR technique. First, 3D image reconstruction was performed by the VR technique from raw image data of 3D FIESTA-C. In this process, window level and width were adjusted visually and manually so that we could recognize the surface shape of soft tissue along the overall head and face. Next, the whole volume of the VR image was inverted from black to white. By doing this, the signal intensity in the cortical bone was converted from black bone to high-signal-intensity bright bone. Similarly, the signal intensity of air space was also converted to a high-signal-intensity area. As a result, both air and cortical bone were inverted to a strong bright-white intensity, whereas the soft tissue along the face and head became a black signal intensity. Next, by cutting out the bright signal intensity area of air (the outermost layer in 3D volume) in a manual fashion, a 3D bone image could be successfully obtained. In this process, the manual procedure was easily performed in all cases because the three layers—air (the

outermost layer), facial soft tissue (the gap area between air and cortical bone) and bone surface—were clearly divided by their different signal intensities. This whole bone reconstruction process is summarized in Fig. 1. An example of 3D-bone image is presented in Fig. 2. In addition, 3D VR imaging with both vessel and bone depiction from the 3D-CTA dataset was also created using the traditional VR technique with the threshold processing method [14]. All 3D reconstruction procedures in both CT and MRI were performed manually to visualize vessel and bone structure as clearly as possible, in the typical clinical manner.

Visual evaluation

After randomizing all MR and CT based bone–vessel VR images, the degree of visualization of the STA branches on each VR image was independently evaluated by three radiological technologists with 14, 20 and 25 years of experience, respectively. The depiction of STA was determined based on a four-grade (0, poor depiction; 1, moderate depiction; 2, good depiction; 3 excellent depiction) system. Each grade was explained as follows: 0, almost no depiction; 1, only the proximal portion was depicted; 2, all portions were depicted, but the depiction of the distal portion was observed to be weak; 3, all parts were well depicted. Representative cases are presented in Fig. 3 and

were given to the scorers as references. Evaluated vessels were the four major STA branches: the right frontal, left frontal, right parietal and left parietal. In each branch, the mean score of the three evaluators for each modality was calculated. To avoid any bias in the scoring of different images, those who had no experience of MR-based vessel bone fusion images were chosen as raters. Additionally, they were blind to all information including study purpose and were simply asked to score the depiction of arteries without any other information.

Statistical analysis

Visual scores of each STA branch (right frontal, left frontal, right parietal and left parietal branch) by the bone–vessel VR images obtained by MR and CT techniques were compared using the Wilcoxon signed-rank test. In addition, interobserver agreement in all pairs among the three radiological technologists was analyzed using kappa (κ) statistics, with the following criteria: 0–0.2, poor agreement: 0.21–0.4, fair agreement: 0.41–0.6, moderate agreement: 0.61–0.8, good agreement, 0.81–1.0, excellent agreement. The level of statistical significance was set at $p<0.05$.

Results

All VR processing using 3D FIESTA-C and TOF-MRA was performed, resulting in coherent 3D bone–vessel VR images for all patients.

In the visual score comparison of MR and CT based bone–vessel VR images of STA branches, the score of right frontal branch MR-based VR image (2.2±0.9) was significantly larger than that for the respective CT image (1.8±0.7) ($p<0.01$). The score of the left frontal branch VR image was also larger for MR than CT (1.9±0.7 v. 1.3±0.8; $p<0.01$). The score of both right and left parietal branches tended to be larger for MR-based than CT-based VR images, but not significantly so ($p=0.06$, 0.13 respectively). A summary of the comparison of visual scores is presented in Table 2. As a detail of the data, all scores in three raters for all the patients were presented in Supplemental Table 1-4. Representative images highlighting marked differences in STA branch depiction between VR images based on MR and CT are presented in Fig. 4. In addition, other nine cases with various degree of the difference of in STA branch depiction were presented in Fig. 5.

In the inter-observer agreement analysis, κ values for STA branch evaluation in MR-based VR images were all good. In CT-based VR images, the κ value for the evaluation of three branches (right frontal, right and left parietal branch) was good (0.60-0.76), but only a moderate κ value (0.5) was observed in the evaluation of the left

frontal branch. All κ values are summarized in Table 3.

Discussion

In the current study, MR-based 3D skull images could be successfully obtained utilizing the signal reverse of 3D FIESTA-C for a 3D VR reconstruction technique. In addition, preoperative bone–vessel VR images for the IC-EC bypass were also successfully obtained with the 3D fusion of MR-based 3D skull images and TOF-MRA. The depiction of STA branches on this MR-based bone–vessel VR image was deemed superior to that of CT-based images in the visual assessment. The depiction of STA branches in the CT-based bone–vessel VR images in this study suffered from the beam hardening effect from the high CT value of the skull, resulting in worse image quality. Compared to such CTA-based 3D bone–vessel VR imaging, TOF-MRA could achieve a clear depiction of STA branches without a beam hardening artifact.

A previous report described that the combination of CT as 3D skull image and TOF-MRA as 3D angiographic image using the bone–vessel fused image played an important role as a navigation tool for the less invasive surgical procedure of STA-MCA bypass with a minimal incision [15]. Compared to this previous report, the current study achieved 3D bone–vessel VR imaging with superb visibility of STA branches using the

non-invasive MR technique only; this technique will provide sufficient vascular anatomical information as a preoperative assessment for STA-MCA bypass surgery with complete non-invasiveness. In particular, this imaging technique is expected to be useful in the evaluation of running vessels around bones other than the skull in the whole body such as the spine, arm and foot area. Black bone MRI derived 3D bone-vessel fused images can play an important role as supplemental pre-operative information for other lesions.

Black-bone MRI acquisition first described by Eley et al. used the parameter settings of a 3D gradient echo sequence with a proton-density weighted imaging like contrast [6]. Their scanning time was described as around 4 minutes. Compared to this, we used the FIESTA-C sequence of b-SSFP technique to obtain both high SNR and a shorter scanning time. Especially, recent MR scanners have been developed to allow the parameter settings with much shorter TR and TE; such developments could lead to more stable image quality of the b-SSFP sequence. In the current study, we could successfully perform acquisition of black-bone MRI with around 3-minute scanning with sufficient VR image visibility. We believe the 3D VR image obtained by our FIESTA-C sequence design can be used to achieve almost the same image quality with a short scanning time compared to the previously reported 3D gradient echo sequence technique [6-9].

The present study has several limitations. First, it was a retrospective study, and thus the patient number was quite small. Second, we used the basic sequence of FIESTA-C for the acquisition of black-bone MRI to obtain a high SNR image with short scanning time; however, direct comparison to the previously reported method described by Eley et al. was not performed. Further analyses to address these limitations will be needed. A third limitation was that we didn't use the source axial images for the evaluation of vessel depiction in both MR and CT, but only used 3D reconstructed images. A combination of 2D source images and 3D reconstructed fusion images may enable the evaluation of vessel depiction in greater detail. Further analysis will be required to resolve this issue. Fourth, arterial arrival timing of contrast agent in CTA was determined by focusing on the depiction for intracranial arteries. This was slightly different from the best timing for the depiction of branches of the external carotid artery. However, we consider that the arterial arrival timing between the main trunk of the STA and the peripheral portion of the intracranial arteries was not largely different unless severe stenosis was observed. Additionally, routine head CTA is generally performed to depict the intracranial arteries; depiction of the external carotid arteries is considered optional. CTA acquisition with the best timing of contrast agent arrival to the external carotid arteries is not realistic in daily clinical practice.

In conclusion, MR bone–vessel fused VR images could be successfully obtained with complete non-invasiveness using FIESTA-C-based black-bone MRI and TOF-MRA. The visibility of STA frontal branches was superior by MR-based bone–vessel VR imaging compared to the 3D-CTA based VR image. This technique may be clinically useful for the preoperative evaluation of donor branches for STA-MCA bypass surgery as a non-invasive method.

References

1. Batjer H, Mickey B, Samson D. Potential roles for early revascularization in patients with acute cerebral ischemia. Neurosurgery 1986;18(3):283-291.

2. Onesti ST, Solomon RA, Quest DO. Cerebral revascularization: a review. Neurosurgery 1989;25(4):618-628; discussion 628-619.

3. Neff KW, Horn P, Dinter D, Vajkoczy P, Schmiedek P, Duber C. Extracranial-intracranial arterial bypass surgery improves total brain blood supply in selected symptomatic patients with unilateral internal carotid artery occlusion and insufficient collateralization. Neuroradiology 2004;46(9):730-737.

4. Nawfel RD, Young GS. Measured Head CT/CTA Skin Dose and Intensive Care Unit Patient Cumulative Exposure. AJNR Am J Neuroradiol 2017;38(3):455-461.

5. Fushimi Y, Miki Y, Kikuta K, Okada T, Kanagaki M, Yamamoto A, et al. Comparison of 3.0- and 1.5-T three-dimensional time-of-flight MR angiography in moyamoya disease: preliminary experience. Radiology 2006;239(1):232-237.

6. Eley KA, McIntyre AG, Watt-Smith SR, Golding SJ. "Black bone" MRI: a partial flip angle technique for radiation reduction in craniofacial imaging. The

Br J Radiol 2012;85(1011):272-278.

7. Eley KA, Watt-Smith SR, Golding SJ. "Black bone" MRI: a potential alternative to CT when imaging the head and neck: report of eight clinical cases and review of the Oxford experience. Br J Radiol 2012;85(1019):1457-1464.

8. Eley KA, Watt-Smith SR, Golding SJ. "Black Bone" MRI: a potential non-ionizing method for three-dimensional cephalometric analysis--a preliminary feasibility study. Dentomaxillofac Radiol 2013;42(10):20130236.

9. Eley KA, Watt-Smith SR, Sheerin F, Golding SJ. "Black Bone" MRI: a potential alternative to CT with three-dimensional reconstruction of the craniofacial skeleton in the diagnosis of craniosynostosis. Eur Radiol 2014;24(10):2417-2426.

10. Eley KA, Watt-Smith SR, Golding SJ. Three-Dimensional Reconstruction of the Craniofacial Skeleton With Gradient Echo Magnetic Resonance Imaging ("Black Bone"): What Is Currently Possible? J Craniofac Surg 2017;28(2):463-467.

11. Dremmen MHG, Wagner MW, Bosemani T, Tekes A, Agostino D, Day E, Soares BP, Huisman T. Does the Addition of a "Black Bone" Sequence to a Fast Multisequence Trauma MR Protocol Allow MRI to Replace CT after Traumatic

Brain Injury in Children? AJNR Am J Neuroradiol 2017;38(11):2187-2192.

12. Scheffler K, Lehnhardt S. Principles and applications of balanced SSFP techniques. Eur Radiol 2003;13(11):2409-2418.

13. Chavhan GB, Babyn PS, Jankharia BG, Cheng HL, Shroff MM. Steady-state MR imaging sequences: physics, classification, and clinical applications. Radiographics 2008;28(4):1147-1160.

14. Fishman EK, Ney DR. Advanced computer applications in radiology: clinical applications. Radiographics 1993;13(2):463-475.

15. Fischer G, Stadie A, Schwandt E, Gawehn J, Boor S, Marx J, et al. Minimally invasive superficial temporal artery to middle cerebral artery bypass through a minicraniotomy: benefit of three-dimensional virtual reality planning using magnetic resonance angiography. Neurosurg Focus 2009;26(5):E20.

Table and Figure Captions

Table 1. Parameters for the acquisition of 3D FIESTA-C

Table 2. Scores in the visual evaluation of STA branches

285

286 **Table3. The mean κ values in visual evaluation among raters**

287

288 **Supplemental Table 1. Scores in the visual evaluation of right frontal branch for all**

289 **the patients**

290

291 **Supplemental Table 2. Scores in the visual evaluation of left frontal branch for all**

292 **the patients**

293

294 **Supplemental Table 3. Scores in the visual evaluation of right parietal branch for**

295 **all the patients**

296

297 **Supplemental Table 4. Scores in the visual evaluation of left parietal branch for all**

298 **the patients**

299

300

301 **Fig. 1. 3D-reconstruction process of the black bone MRI**

First, 3D image was reconstructed with the volume rendering (VR) process from raw image data of 3D FIESTA-C (black arrow). Next, the whole volume of the VR image was inverted from black to white (gray arrow). After this process, both air and cortical bone were inverted to a strong bright-white intensity, whereas the soft tissue along the face and head became a black signal intensity. The bright signal intensity area of air (the outermost layer in 3D volume) was carefully cut with manual fashion (white arrow), a 3D bone image could be obtained (arrowhead).

Fig. 2. MR-reconstructed 3D-volume rendering skull image

Example of 3D VR bone–vessel fused image obtained from the FIESTA-C sequence is presented. Clear depictions of the bone structure were observed from all three directions.

Fig. 3. Reference cases for four-grade system in visual evaluation

Reference cases of four-grade (0, 1, 2 and 3) system for the evaluation of the parietal branch were presented. Poor depiction (grade 0): almost no depiction of parietal branch (a, arrow), moderate depiction (grade 1): only the proximal portion was depicted (b, arrow), good depiction (grade 2): all portions were depicted, but the depiction of the

distal portion was observed to be weak (c, arrow), excellent depiction (grade 3): all parts were well depicted (d, arrow).

Fig. 4. A case example of marked visualization difference of STA branches

In MR-based bone–vessel fused image (a), the frontal branch of the STA was well visualized (a: arrowhead). In contrast, in the CT-based bone–vessel fused image (b), the same part of the frontal branch was not clearly observed (b: arrowhead).

Fig. 5. Nine cases with various degree of the difference of in STA branch depiction

Nine cases of CT-based (left side) and MR-based (right side) 3D volume-rendering bone-vessel fused images are presented (a-i). Overall, the depiction of the peripheral portion of the STA on MR-based VR images was visually superior to that of CT-based VR.

Table 1. Parameters for the acquisition of 3D FIESTA-C

matrix	384×320
field of view [cm]	22
slice thickness [mm]	1.4
TR [ms]	4.6-4.8
TE [ms]	1.7-1.8
bandwidth [kHz]	90.91
slice number	200
ZIP	2
ARC factor	1.75×1.75
scan time	3’03

FOOTNOTE: ZIP, zero fill interpolation; ARC, autocalibrating reconstruction for cartesian imaging (Phase×Slice)

Table 2. Scores in the visual evaluation of STA branches

Name of branch	CT	MR
Right frontal branch	1.8±0.7	2.2±0.9*
Left Parietal branch	1.8±1.0	2.1±0.8
Right frontal branch	1.3±0.8	1.9±0.7*
Left parietal branch	2.5±0.6	2.6±0.7

*P<0.05

FOOTNOTE : STA, superficial temporal artery

Table3. The mean κ values in visual evaluation among raters

	CT	MR
Frontal branch (right)	0.67	0.60
Parietal branch (right)	0.67	0.76
Frontal branch (left)	0.50	0.65
Parietal branch (left)	0.65	0.60

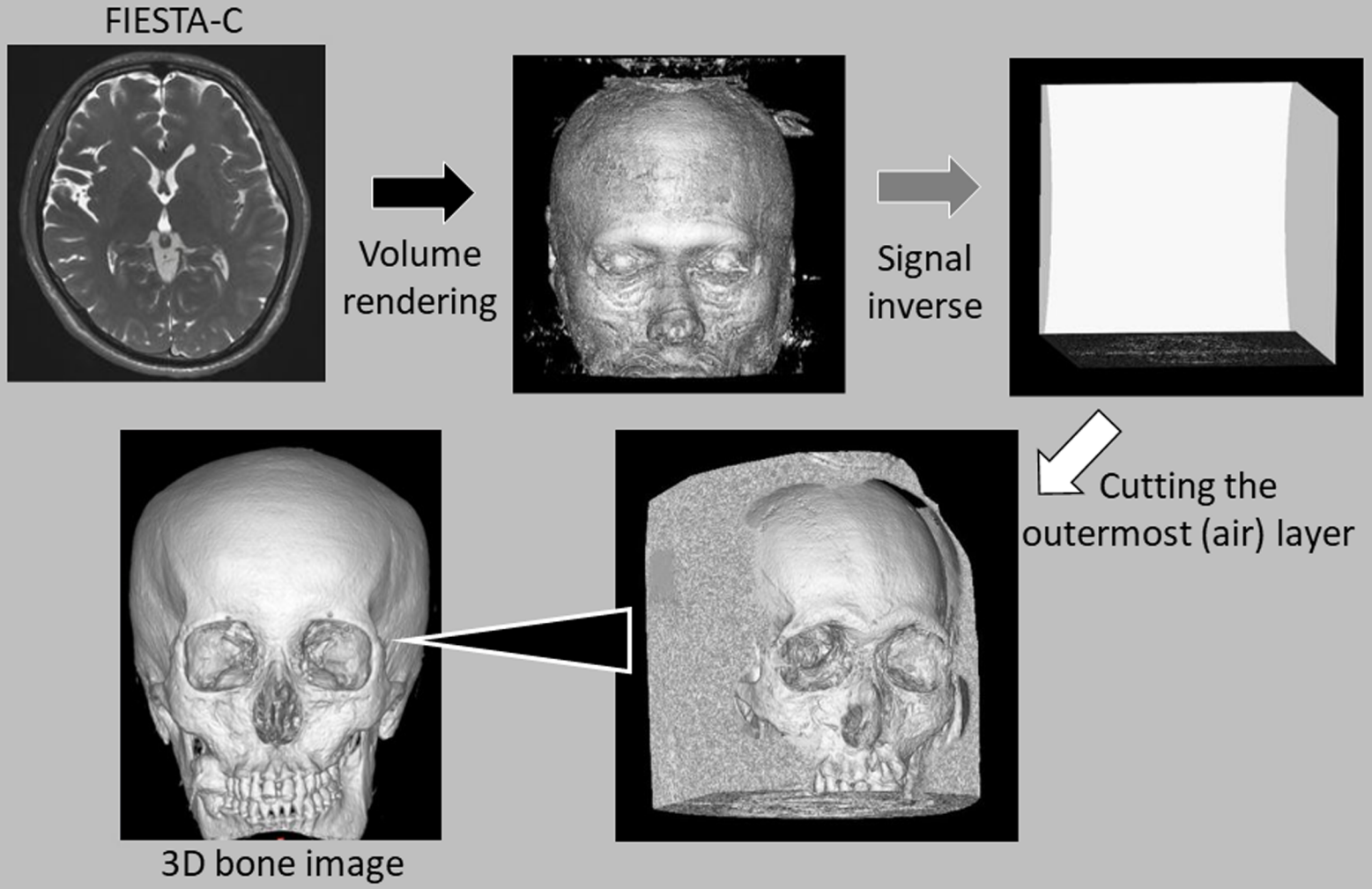
FIESTA-C
Volume rendering
Signal inverse
Cutting the outermost (air) layer
3D bone image

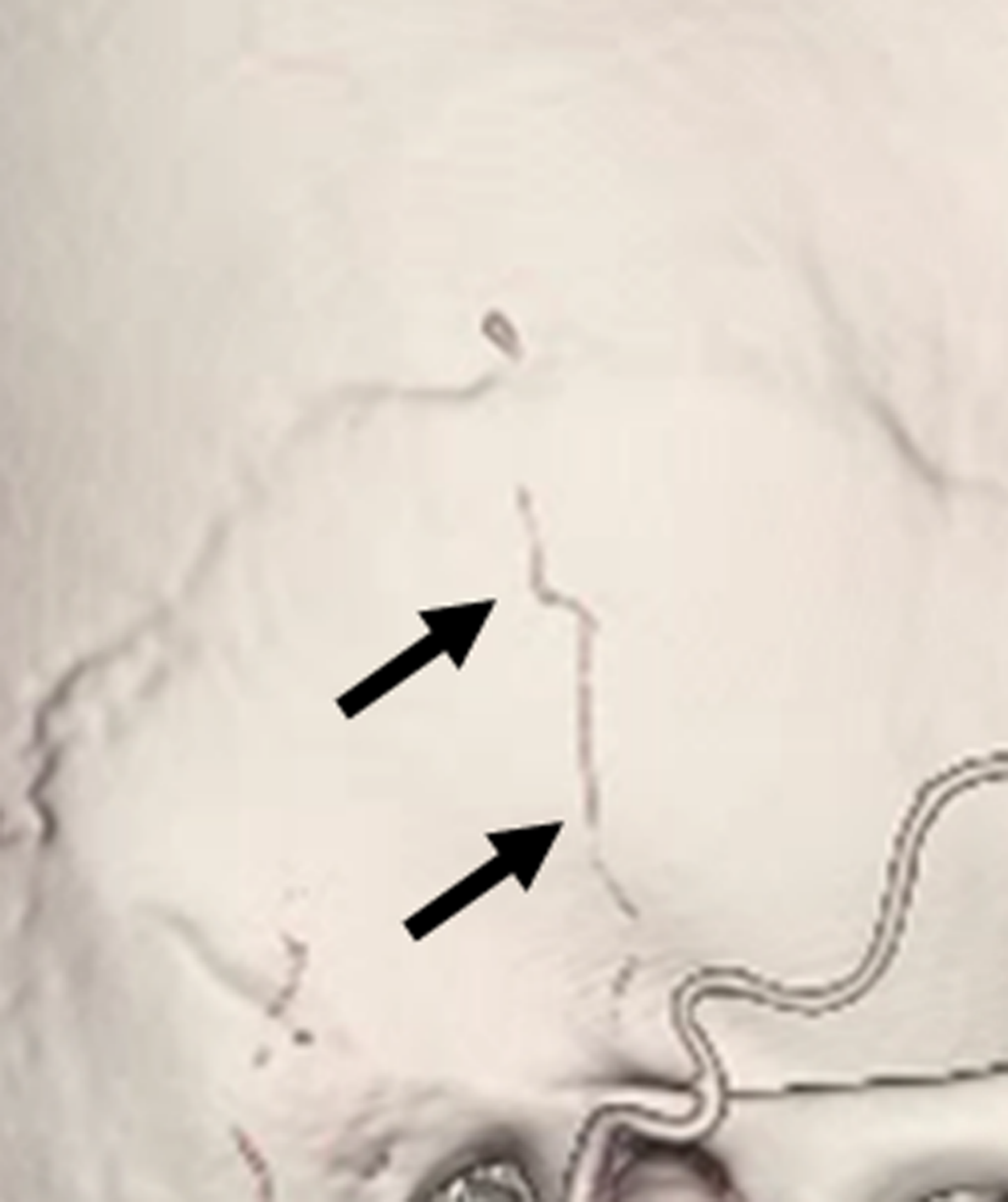

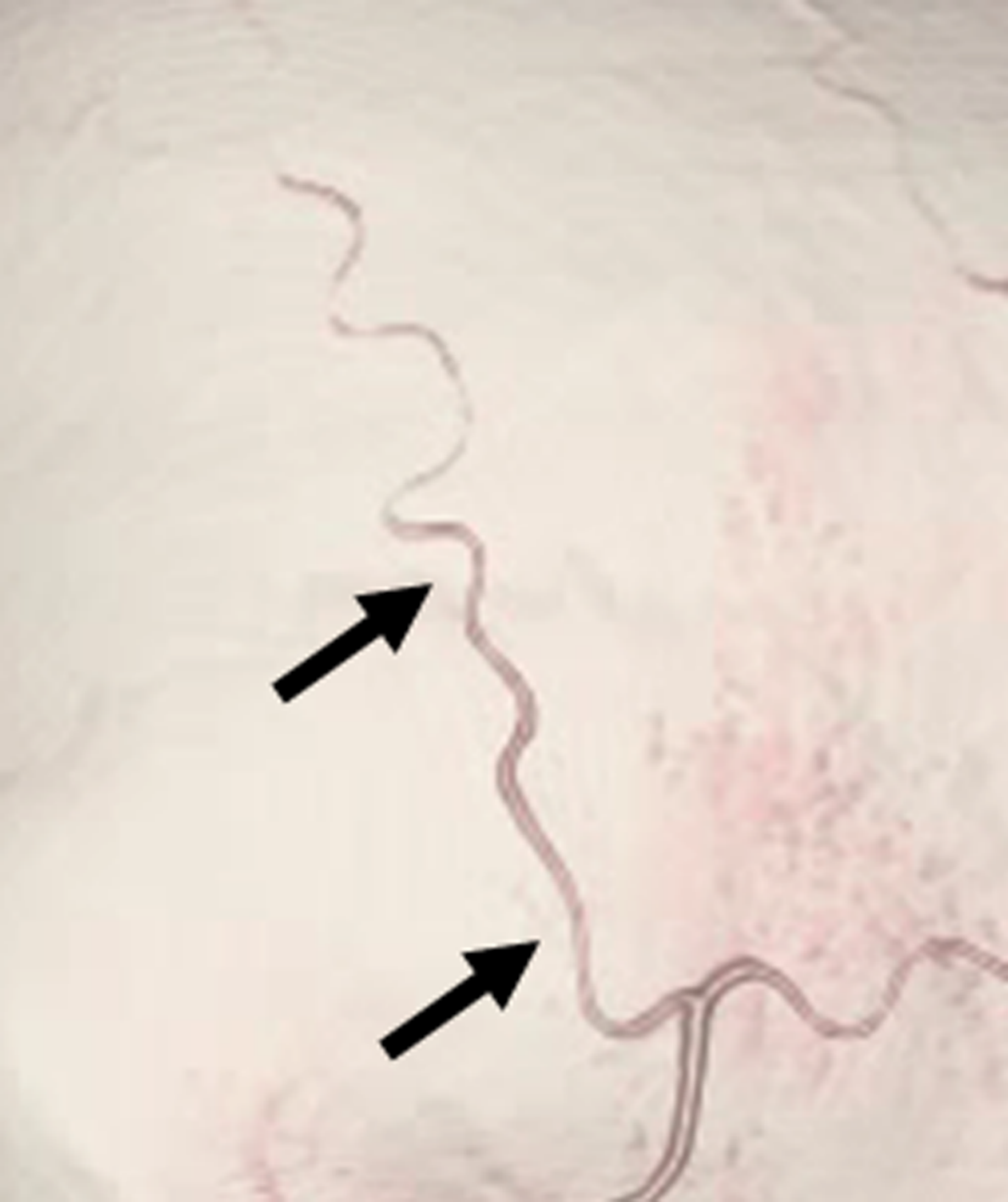

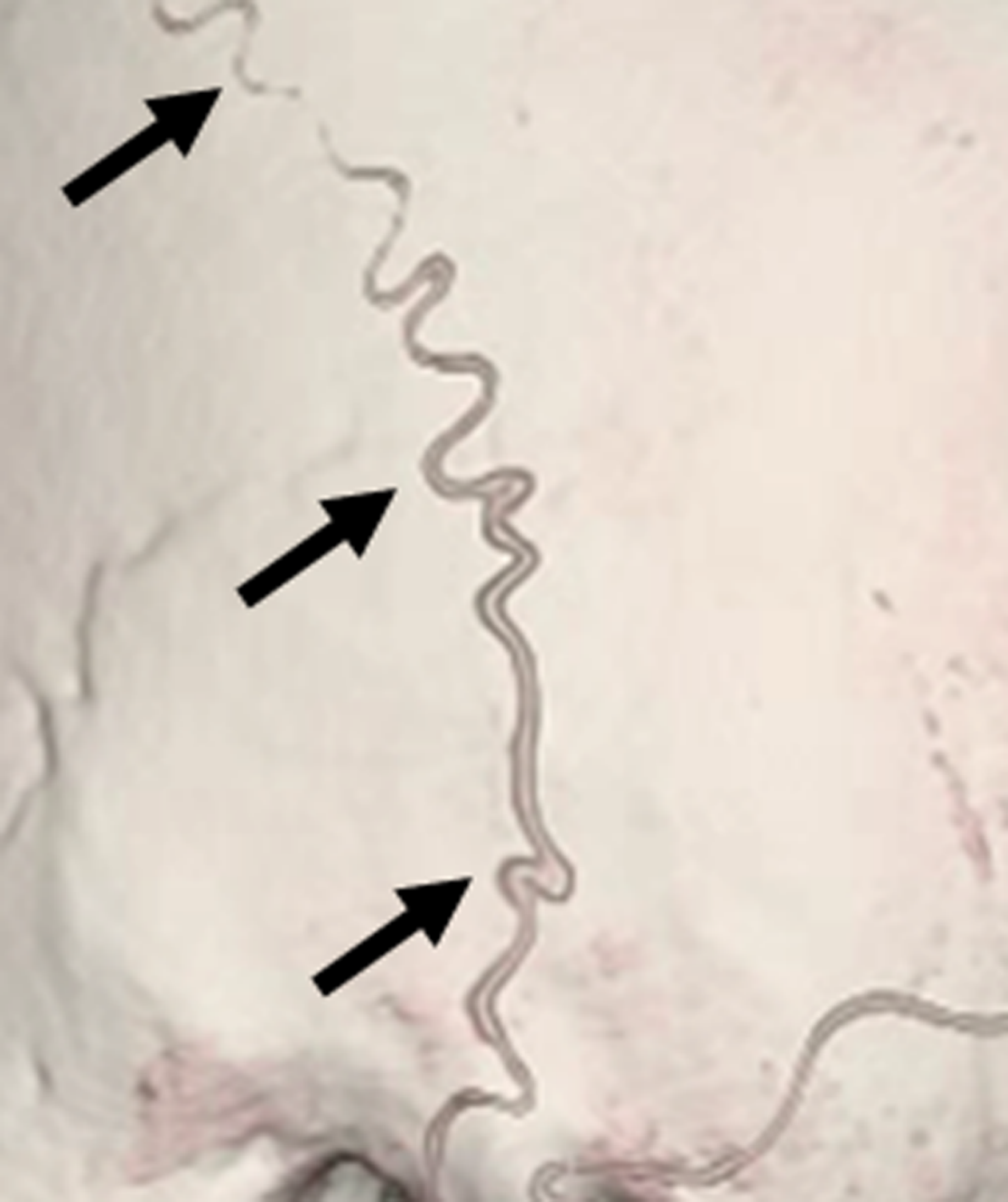

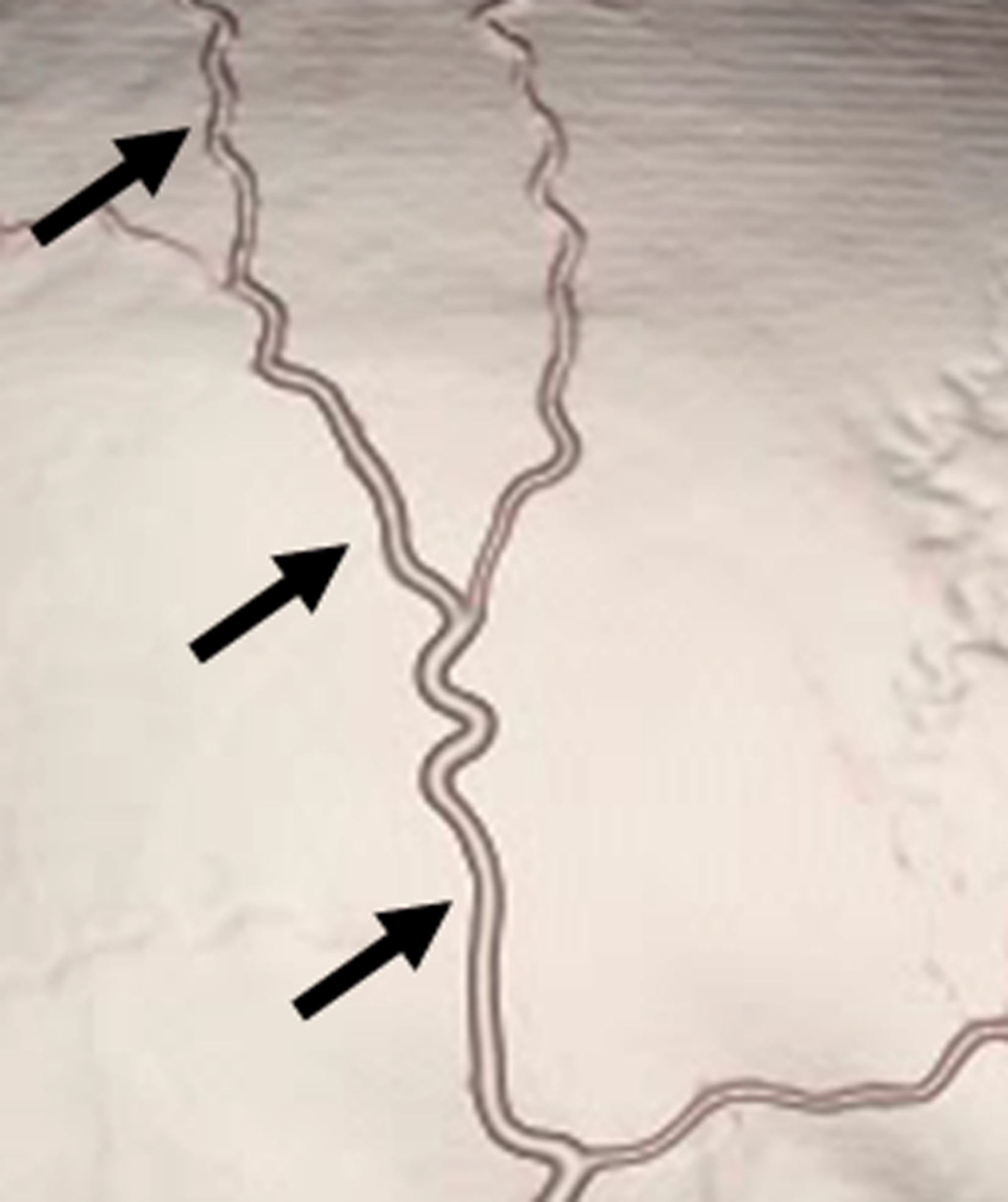

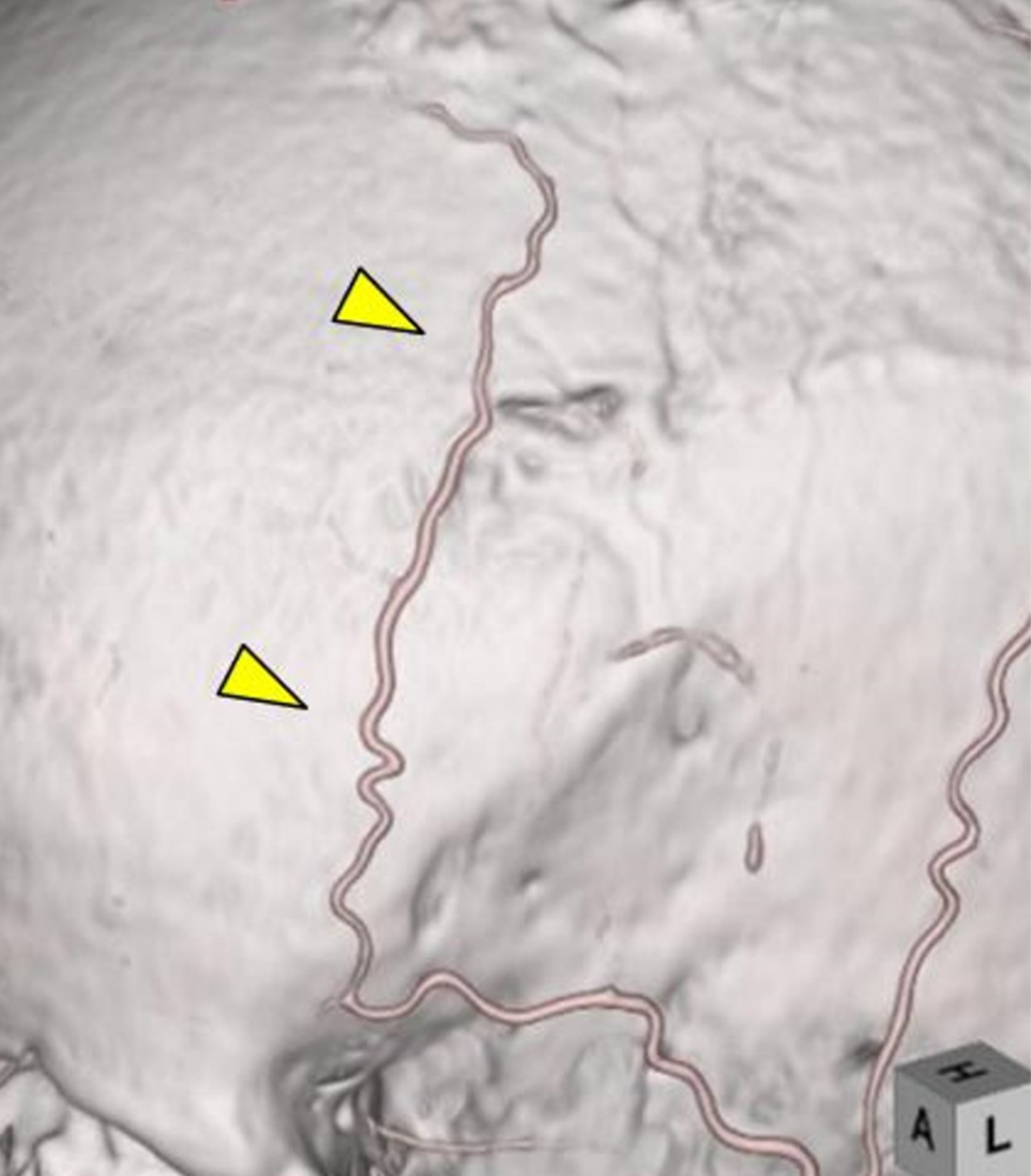
H
A
L

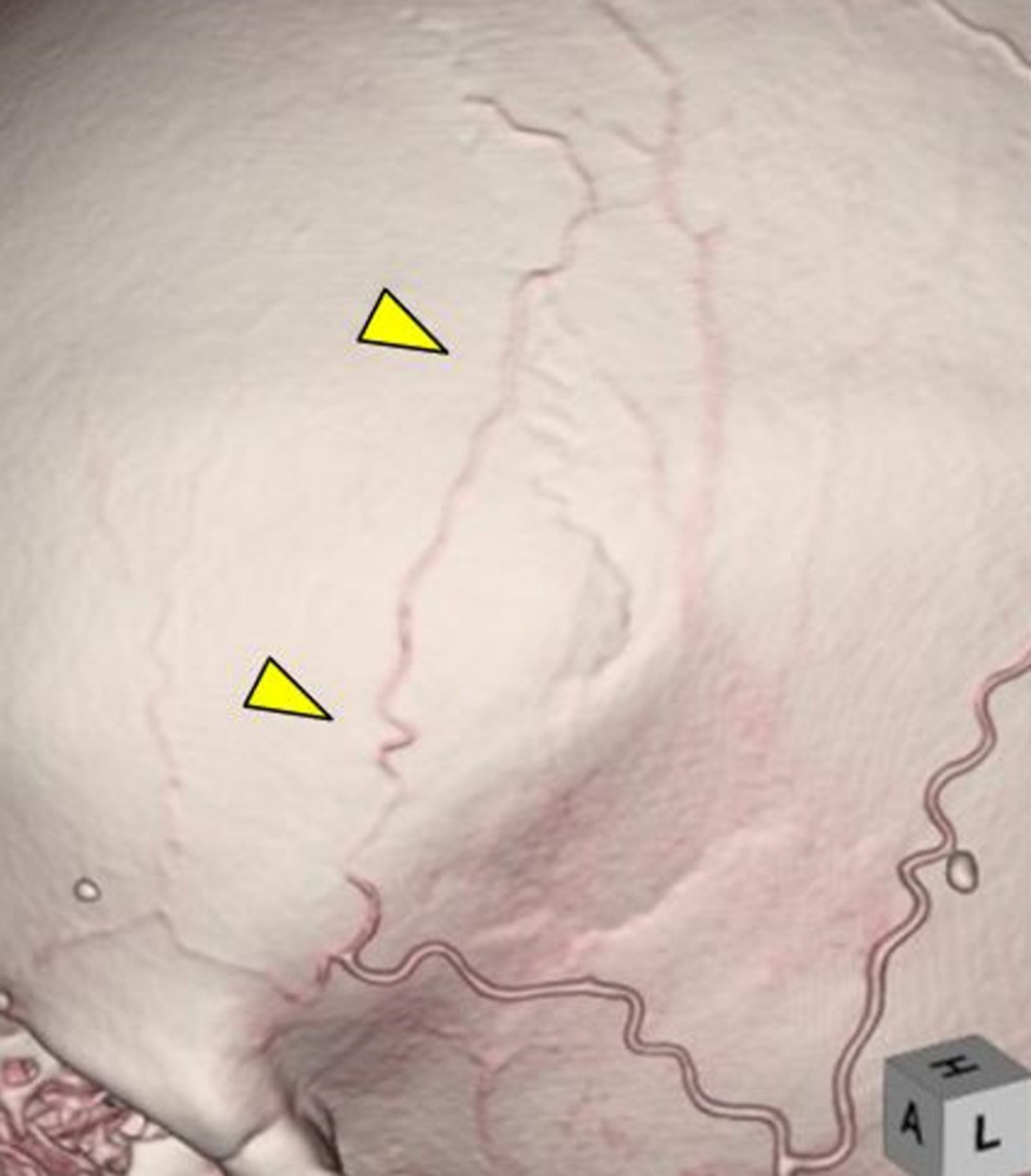
H
A
L